

THE INFLUENCE OF HEIGHT RATIO ON RAYLEIGH-NUMBER SCALING AND STABILITY OF HORIZONTAL CONVECTION

Gregory J SHEARD^{1*} and Martin P. KING²

¹ Fluids Laboratory for Aeronautical and Industrial Research (FLAIR), Department of Mechanical and Aerospace Engineering, Monash University, VIC 3800, AUSTRALIA

² School of Engineering, Sunway Campus, Monash University, Jalan Lagoon Selatan, Bandar Sunway, 46150, Selangor Darul Ehsan, MALAYSIA

*Corresponding author, E-mail address: Greg.Sheard@eng.monash.edu.au

ABSTRACT

Horizontal convection in a rectangular enclosure driven by a linear temperature profile along the bottom boundary is investigated numerically using a high-resolution spectral-element discretization in space and a third-order time integration scheme for velocity and temperature fields. A Boussinesq approximation is employed to model buoyancy.

The emphasis of this study is on the scaling of Nusselt number and boundary layer quantities with aspect ratio and Rayleigh number.

At low Rayleigh number, Nusselt number and boundary-layer thickness are found to be independent of Rayleigh number, but do vary with enclosure aspect ratio. At higher Rayleigh numbers, convective flow dominates, and Nusselt number, boundary layer thickness and peak boundary layer velocity become independent of the enclosure aspect ratio. In this regime, the Rayleigh-number scaling of these quantities agrees well with exponents predicted by theory, with trends consistent with exponents of 1/5, -1/5 and 2/5 for Nusselt number, boundary-layer thickness and boundary-layer velocity, respectively, being found. Unsteady flow develops at a critical Rayleigh number independent of aspect ratio, and the development of unsteady flow is found to lead to an increase in the Nusselt number scaling exponent from 0.2 to approximately 0.3, which is closer to the theoretical upper bound than has yet been reported in the study of horizontal convection flows.

NOMENCLATURE

c_p	specific heat capacity
D	height of enclosure
F_T	heat flux
g	acceleration due to gravity
\mathbf{g}	gravity vector
$\hat{\mathbf{g}}$	unit vector in the direction of gravity
h_{thermal}	height of thermal boundary layer
h_{velocity}	height of velocity boundary layer
L	width of enclosure
Nu	Nusselt number
p	kinematic pressure
Pr	Prandtl number
Ra	Rayleigh number
s	scalar field representing temperature
T	temperature
t	time
\mathbf{u}	velocity vector
u_{max}	maximum velocity in boundary layer

x	horizontal coordinate
y	vertical coordinate
α	thermal expansion coefficient
δT	maximum temperature difference along bottom
κ_T	thermal diffusivity
ρ_0	reference density of fluid
ν	kinematic viscosity

INTRODUCTION

Horizontal convection refers to the heat and fluid flows established in an enclosure due to differential heating along just one horizontal boundary (Hughes & Griffiths 2008). This is in contrast with other forms of convection which are often driven by a temperature differential imposed between two opposite boundaries (see, for instance, Niemela & Sreenivasan 2003). Whether horizontal convection is achieved by an applied horizontal temperature gradient or by an applied heat flux, unstable convective flow is forced in one side of the enclosure while the rest of fluid is convectively stable. Therefore, in contrast to the extensively studied Rayleigh-Bénard convection, whereby both cooling and heating promote convective overturning, the strength of overturning in horizontal convection is ultimately limited by heat diffusion.

Motivation for the study of horizontal convection comes from geophysical and geological flows. For example, despite heavy simplifications, studies into horizontal convection are providing understanding and insight into meridional (North-South) overturning circulation in the oceans, where they are heated and cooled along a thin horizontal layer. Interest in horizontal convection is also emerging amongst researchers including engineers, applied mathematicians and oceanographers. For reviews which discuss recent advances and outstanding questions in this subject, the readers are referred to Hughes & Griffiths (2008); Wunsch & Ferrari (2004), as well as references therein.

In their review article Hughes & Griffiths (2008) describe horizontal convection in detail, but a brief overview is included here. At low Rayleigh numbers, horizontal convection flow is dominated by diffusion, and is stable in time. It comprises a nearly symmetrical overturning circulation of fluid driven by a buoyancy destabilization on the heated boundary with flow moving along the bottom boundary from the cold end to the hot end (or the hot to cold end if the top boundary is the heated boundary). Buoyant fluid then rises (or descends) in a narrow vertical plume, before returning to complete the

circulation in a diffusive horizontal return flow. As the Rayleigh number is increased, studies have shown that convective effects begin to dictate the fluid and heat transfer behaviour, with thermal and velocity boundary layers developing along the heated boundary. Beyond some critical Rayleigh number, the flow eventually becomes unsteady, which is particularly visible in the vicinity of the vertical plume (Mullarney, Griffiths & Hughes 2004). A scaling analysis by Paparella & Young (2002), in which dissipation was shown to vanish as kinematic viscosity and thermal diffusion go to zero, was used to present an argument that horizontal convection was inherently non-turbulent. Regardless of whether the flow is defined as turbulent, it does feature small-scale and irregular, unsteady flow structures convect from the heated wall boundary layer into the vertical plume beyond some critical Rayleigh number.

Experiments by Mullarney *et al.* (2004) with water in an enclosure with height-to-width aspect ratio of 0.16 showed that beyond the diffusion-dominated regime, the Nusselt number scaled with approximately the $1/5^{\text{th}}$ power of Rayleigh number. Siggers, Kerswell & Balmforth (2004) used a variational analysis to determine that an upper bound on Nusselt number scaling was a $1/3^{\text{rd}}$ power of Rayleigh number, though to the authors' knowledge, scaling exponents above $1/5^{\text{th}}$ have not been detected in horizontal convection experiments.

Chiu-Webster, Hinch & Lister (2008) studied horizontal convection in the infinite-Prandtl-number limit relevant to very viscous fluids, at a range of aspect ratios and Rayleigh numbers. That study also found the Nusselt number to scale with the $1/5^{\text{th}}$ power of Rayleigh number, and presented evidence of an aspect-ratio-independence beyond Rayleigh numbers of approximately 10^7 .

Despite these past investigations, the aspect-ratio-dependence of features such as the transition to the convection-dominated regime, and the onset of unsteady flow remain poorly understood. In this paper we investigate the effect of the aspect ratio of the enclosure on the scaling relationships for heat transfer, boundary layer thicknesses, boundary-layer velocities, and the transition to unsteady flow.

MODEL DESCRIPTION

Problem Definition

The problem considered in this paper is the two-dimensional horizontal convection of fluid in a rectangular enclosure of width L and height D . The flow is driven by a linear temperature profile applied along the bottom wall of the enclosure, as illustrated in figure 1. The side and top walls are insulated (a zero temperature gradient is imposed normal to the walls), and a no-slip condition is imposed on the velocity field on all walls.

A Boussinesq approximation of the fluid buoyancy is employed, whereby density differences in the fluid are neglected with the exception of the gravity contribution. A scalar field representing the fluid temperature (which relates linearly to the density via a thermal expansion coefficient, α) is evolved via an advection-diffusion operation in conjunction with the velocity field.

Governing Equations and Parameters

The equations governing a Boussinesq fluid may be written as

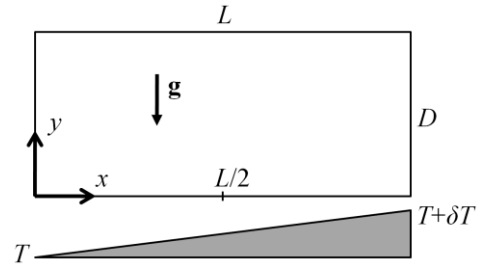


Figure 1: A schematic diagram of the system. The origin of the coordinate system is positioned at the bottom-left corner, gravity acts vertically downward, and a temperature difference of δT is imposed along the bottom wall.

$$\frac{\partial \mathbf{u}}{\partial t} = -(\mathbf{u} \cdot \nabla) \mathbf{u} - \nabla p + Pr \nabla^2 \mathbf{u} - Pr Ra \hat{\mathbf{g}} s, \quad \nabla \cdot \mathbf{u} = 0, \quad (1)$$

$$\frac{\partial s}{\partial t} = -(\mathbf{u} \cdot \nabla) s + \nabla^2 s,$$

where \mathbf{u} is the velocity vector, p the kinematic static pressure, t is time, Ra is the Rayleigh number, Pr the Prandtl number, $\hat{\mathbf{g}}$ a unit vector in the direction of gravity, and s is a scalar field representing temperature.

In equation (1), lengths have been scaled by the enclosure width L , velocities by L/κ_T (where κ_T is the thermal diffusivity of the fluid), time by κ_T/L^2 , and temperature by δT (the imposed temperature difference imposed across the bottom wall). The (horizontal) Rayleigh number is defined as

$$Ra = \frac{g \alpha \delta T L^3}{\nu \kappa_T},$$

where g is the acceleration due to gravity and ν is the kinematic viscosity of the fluid.

If a heat flux is defined as

$$F_T = \kappa_T \rho_0 c_p \frac{\partial T}{\partial y},$$

where ρ_0 is a reference fluid density, c_p the specific heat capacity of the fluid, $\partial T / \partial y$ is the mean temperature gradient along the bottom wall over $0 \leq x \leq L/2$, then a flux Rayleigh number may be defined as

$$Ra_F = \frac{g \alpha F_T L^4}{\rho_0 c_p \kappa_T^2 \nu}.$$

In the experimental study by Mullarney *et al.* (2004), horizontal convection was driven by applying a heat flux over half of the bottom wall, and a constant temperature along the other half. Those flows were conveniently scaled using the flux Rayleigh number, whereas the horizontal Rayleigh number (Ra) is more appropriate to use for horizontal convection driven using a linear temperature profile as applied in the present study.

The relationship between fluid viscosity and thermal diffusivity is parameterized by the Prandtl number

$$Pr = \frac{\nu}{\kappa_T}.$$

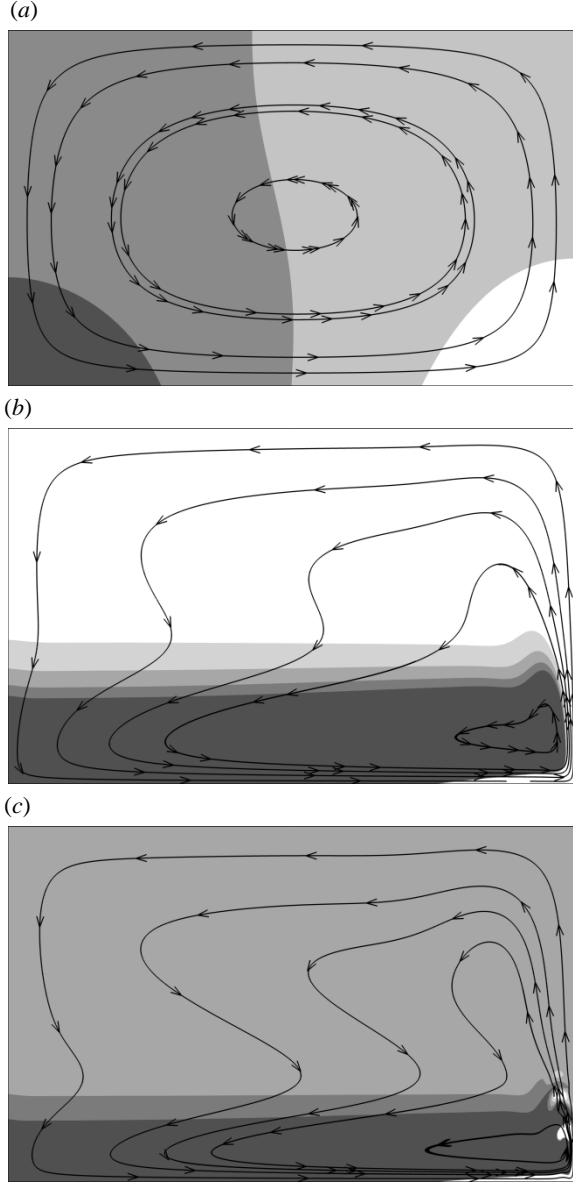


Figure 2: Contour plots of temperature overlaid with velocity streamlines for horizontal convection in an enclosure with $D/L = 0.625$ at Rayleigh numbers $Ra =$ (a) 1.43×10^3 , (b) 1.43×10^8 and (c) 1.43×10^9 . Light and dark shading represents cool and warm fluid, respectively, and contour levels are arbitrarily chosen to elucidate flow features in the enclosure.

Throughout this study the Prandtl number is maintained at $Pr = 6.14$, consistent with water at room temperature.

Finally, the Nusselt number represents the ratio of convective to conductive heat transfer, and may be defined as

$$Nu = \frac{F_T L}{\rho_0 c_p \kappa_T \delta T}$$

Numerical Approach

The Boussinesq flow described by equation (1) is computed using a high-order in-house solver which employs a spectral-element method for spatial discretization and a third-order backward multi-step method for time integration (Sheard *et al.* 2007; Sheard, Fitzgerald & Ryan 2009). This scheme is used to evolve

both the velocity and scalar (temperature) fields. The present study spans a very wide range of Rayleigh number, which for higher Rayleigh number placed considerable limitations on permissible time steps. Beyond $Ra \approx O(10^3)$, the maximum allowable time step in the computations scaled approximately with $1/Ra$. Following the boundary- and thermal-layer scaling analysis of Mullarney *et al.* (2004), higher spatial resolution was also required as fluid scales reduced with increasing Ra .

RESULTS

With an increase in Rayleigh number, the horizontal convection flow passes from a diffusion-dominated regime to a steady-state convection-dominated regime, before subsequently developing unsteady flow, which is concentrated in the vicinity of the vertical plume rising from the hot end of the heated boundary. Figure 2 plots temperature contours and streamlines for horizontal convection in an enclosure with $D/L = 0.625$ in each of these regimes.

The same progression through these regimes was found for all enclosure proportions in the range investigated, $0.16 \leq D/L \leq 2$, though the Rayleigh numbers marking the transition between neighbouring regimes do exhibit a dependence on D/L , which will be explored subsequently. Flows are computed in this study over a wide range of Rayleigh numbers $4.36 \times 10^{-4} \leq Ra \leq 8.52 \times 10^{11}$

The quantities of most interest in horizontal convection are the Nusselt number, the thermal and velocity boundary-layer thicknesses, and the peak velocity within the boundary layer adjacent to the heated boundary. Mullarney *et al.* (2004) proposed scalings for these quantities with flux Rayleigh number (Ra_F), given as

$$Nu \sim Ra_F^{1/6},$$

$$UL/\kappa_T \sim Ra_F^{1/3},$$

$$h/L \sim Ra_F^{-1/6}.$$

In the present study, convection is controlled not by the flux Rayleigh number, but by the horizontal Rayleigh number Ra , and thus the expected scaling are recast as

$$Nu \sim Ra^{1/5},$$

$$UL/\kappa_T \sim Ra^{2/5},$$

$$h/L \sim Ra^{-1/5}.$$

The Nusselt number may be calculated in the present configuration after calculating the heat flux (F_T) along the cooler half of the heated boundary, as defined in the Introduction. The calculated Nusselt numbers are plotted against Rayleigh number in figure 3. The plot shows that at low Rayleigh number, the Nusselt number is independent of Rayleigh number, but is a function of D/L , with Nu decreasing with decreasing D/L . As Ra is increased, the data for each aspect ratio collapse onto a single trend, which is nearly linear on a log-log plot, with a gradient of $1/5$. This gradient is consistent with the theoretical scaling from Mullarney *et al.* (2004). The trend in figure 3 exhibits a slight increase in gradient beyond approximately $\log(Ra) \approx 9.5$. It is noted that this corresponds to the development of unsteady flow in the enclosure.

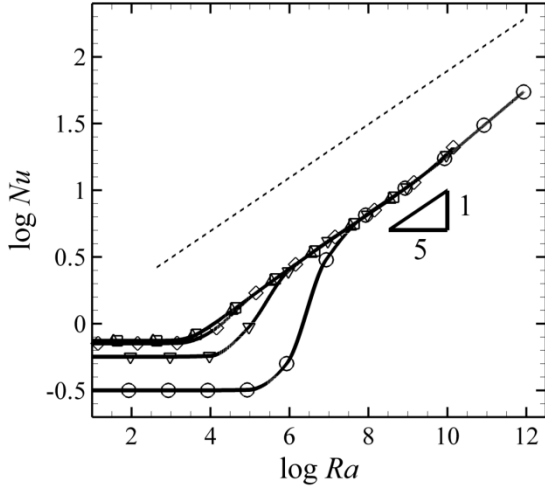


Figure 3: A plot of $\log(Nu)$ against $\log(Ra)$, for $D/L = 2$ (\square), 1 (Δ), 0.625 (\diamond), 0.333 (∇), and 0.16 (\circ). Akima splines are fitted to the data for guidance. A dotted line shows the empirical trend proposed by Mullarney *et al.* (2004). Note that a base-10 logarithm is used in all plots in this study.

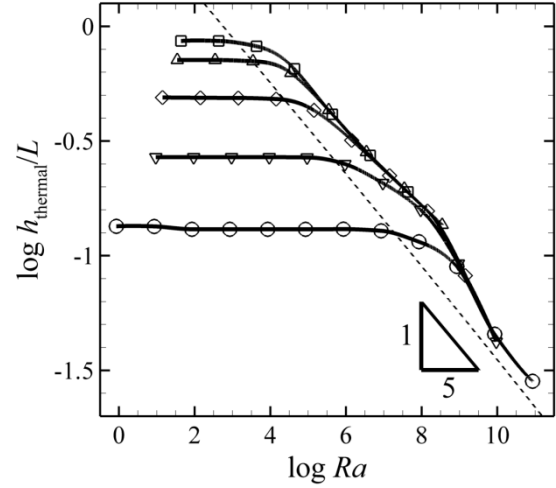


Figure 5: A plot of $\log(h_{\text{thermal}}/L)$ against $\log(Ra)$ for various D/L . Symbols are as per figure 3. The dotted line shows the empirical trend proposed by Mullarney *et al.* (2004), and a gradient of $-1/5$ is provided for comparison with theory.

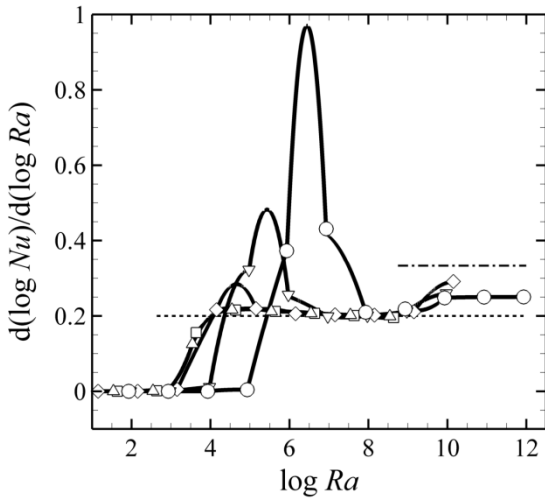


Figure 4: A plot of the gradient of the $\log(Nu)$ - $\log(Ra)$ curves from figure 3. Gradients are calculated from finely discretized Akima splines fitted to the data. A dotted line illustrates the theoretical gradient of $1/5$ reported by Mullarney *et al.* (2004), and a dash-dot line shows the theoretical upper bound proposed by Siggers *et al.* (2004).

To further elucidate the scaling of the data shown in figure 3, gradients were computed by fitting Akima splines to the data (Akima splines are less susceptible to the wiggle artefacts which affect other curve-fitting functions such as polynomial interpolation or cubic splines), and calculating the gradients using finite differences. This data is plotted in figure 4. In enclosures with approximately $D/L \geq 1$, the gradient increases from zero to $1/5$ at $\log(Ra) \approx 4$. With decreasing D/L , the collapse to the gradient of $1/5$ occurs at higher Ra ; i.e., at $D/L = 0.16$, $\log(Ra) \approx 8$.

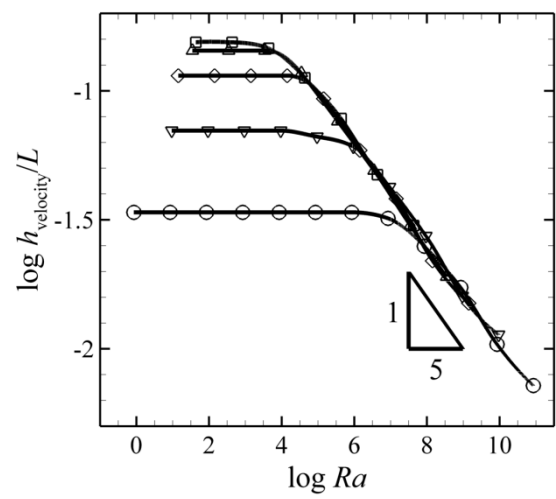


Figure 6: A plot of $\log(h_{\text{velocity}}/L)$ against $\log(Ra)$ for various D/L . Symbols are as per figure 3, and a gradient of $-1/5$ is provided for comparison with theory.

Figure 4 confirms that beyond $\log(Ra) \approx 9.5$, the calculated gradients increase from approximately 0.2 to values in the range 0.25 to 0.30. This is a significant observation, as such a gradient was not detected in the measurements of Mullarney *et al.* (2004), yet Siggers *et al.* (2004) performed an analysis which proposed an exponent of $1/3$ as the upper bound on Nu - Ra scaling for horizontal convection. The elevated gradients detected in these simulations may signify a transition to a previously undetected regime of horizontal convection. The simulations performed in this study employ a higher spatial resolution than that employed in the numerical simulations conducted by Mullarney *et al.* (2004), which may explain why that study did not report scaling

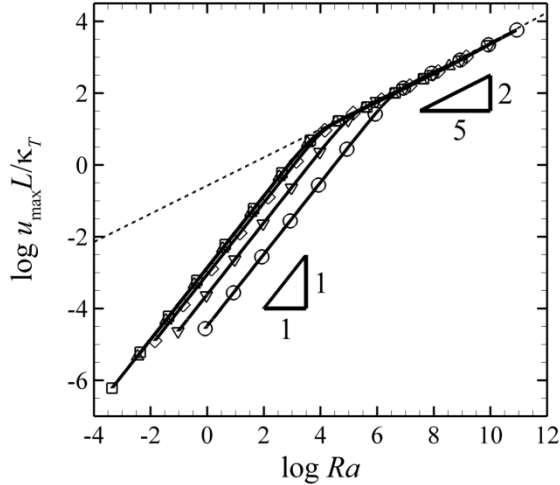


Figure 7: A plot of $\log(u_{\max}L/\kappa_T)$ against $\log(Ra)$ for various D/L . Symbols are as per figure 3. The dotted line shows the empirical trend proposed by Mullarney *et al.* (2004), and a gradient of $2/5$ is provided for comparison with theory.

exponents beyond $1/5$. The increase in gradient detected here occurs as unsteady flow develops in the enclosure shows that heat transfer is enhanced by the development of unsteady flow in this configuration.

Thermal and velocity boundary layer thicknesses are calculated at $x = L/2$. These quantities are plotted against Rayleigh number in figures 5 and 6. The thermal boundary layer thickness is taken to be the point at which the temperature is 5% less than the temperature at the top wall, and the velocity boundary layer thickness is taken to be at the point of maximum velocity in the boundary layer.

In the low-Rayleigh-number diffusion regime, the boundary layer thicknesses are independent of Rayleigh number. In this regime, enclosures with larger D/L have a larger boundary-layer thickness. With increasing Ra , the h_{thermal}/L data overshoots the empirical trend measured by Mullarney *et al.* (2004), before collapsing onto a single trend with a gradient of approximately $-1/5$, consistent with theory. Similar Rayleigh-number dependence and collapse behaviour is observed for h_{velocity}/L in figure 6.

The peak boundary layer velocity on the centreline of the enclosure displays two regimes of linear behaviour with Rayleigh number on a log-log plot as shown in figure 7. For all D/L , a unit gradient is found in the low- Ra regime, which persists to approximately $\log(Ra) \approx 3.5$ to 6.5 for $D/L \approx 2$ down to 0.16 . At higher Rayleigh numbers, the data again collapses to a linear trend, this time with a gradient of $2/5$, which is consistent with theory. Furthermore, the data in this convective regime agrees very well with the empirical trend reported by Mullarney *et al.* (2004).

To characterize the enclosure aspect ratio dependence on transition from the diffusion-dominated regime to the convective regime, a criterion was established whereby deviation of more than 5% from the Ra -independent values of Nu and h_{velocity}/L identified the critical Rayleigh number. Figure 8 plots the critical Rayleigh numbers as a function of D/L for the data shown in figures 3 and 6. It is found that for Nu , the critical Rayleigh number denoting transition to convective flow is insensitive to enclosure

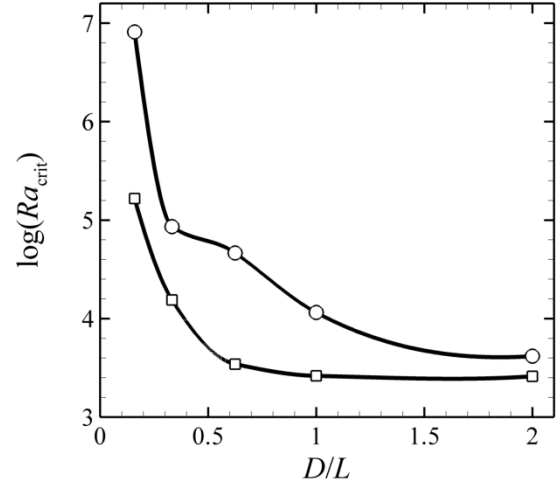


Figure 8: A plot of the logarithm of critical Rayleigh number against D/L , for Nu (\square) and h_{velocity}/L (\circ) data. Curves are spline fits to the data for guidance.

aspect ratio above $D/L \approx 1$. At lower aspect ratios, the critical Rayleigh number increases hyperbolically as $D/L \rightarrow 0$. This trend is shared for the boundary-layer thickness data, though at consistently higher critical Rayleigh numbers, with the exception that above $D/L \approx 1$, the critical Rayleigh number is seen to decrease appreciably with increasing D/L . Due to the sparsity of the original data (h_{velocity}/L was computed at power-of-10 Ra intervals), it is unclear whether the Ra_{crit} data point at $D/L = 0.333$ undershoots an otherwise hyperbolic trend, or whether the low- D/L values of 0.16 and 0.333 form a separate branch to the data at $D/L \geq 0.625$.

It is known that beyond some Rayleigh number in the convective regime, the horizontal convection flow develops unsteady flow. An example of this can be seen in figure 2 *c*, where the vertical plume in the bottom-right corner of the enclosure exhibits a time-dependent pulsing. Similar observations can be made in the visualizations in Mullarney *et al.* (2004). Analysis of time histories of heat flux through the bottom wall permitted the temporal characteristics of the saturated flows computed in this study to be determined. It was found that somewhere in the range $3.5 \times 10^8 < Ra < 8.5 \times 10^8$, the flow transitioned from a steady to a time-dependent state. Figure 9 plots the $\log(Ra)$ - D/L parameter space computed in this study, identifying steady and time-dependent cases. It is found that there exists little or no aspect-ratio dependence on the transition Rayleigh number for unsteady flow. Given that the Nu and boundary-layer data at various D/L have been shown to collapse onto a single curve, implying independence on D/L , it is interesting to observe that a similar independence on enclosure aspect ratio is found for the transition to unsteady flow. This result strongly suggests that the mechanism leading to the transition to unsteady flow is closely tied to the thermal and velocity boundary layers along the heated boundary.

CONCLUSION

Horizontal convection has been computed at high spatial resolution using a spectral-element method, over a wide range of Rayleigh numbers and enclosure aspect ratios, at a Prandtl number of 6.14 , which is consistent with water at room temperature.

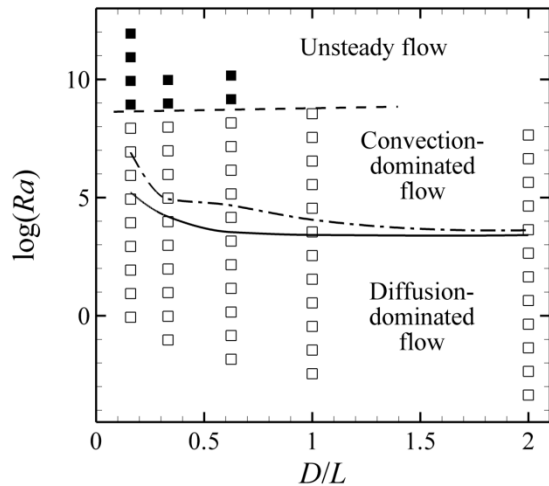


Figure 9: A plot of the $\log(Ra)$ - D/L parameter space computed in this study. Symbols denote points at which data was acquired, with open and filled symbols showing steady and unsteady solutions, respectively. Solid and dash-dot lines reproduce the critical Rayleigh number curves given in figure 8 for comparison, and a dashed line marks the approximate boundary between steady and unsteady regimes.

At low Rayleigh number, the Nusselt number and boundary layer thickness demonstrate Rayleigh-number independence, though they do vary with aspect ratio. Above some critical Rayleigh number, all simulated scalings for Nusselt number, boundary layer thickness, and boundary layer velocity each collapse to single curves independent of aspect ratio, and in agreement with theory, i.e. $Nu \sim Ra^{1/5}$, $h/L \sim Ra^{-1/5}$, and $UL/\kappa_T \sim Ra^{2/5}$, respectively (see figures 3, 5, 6, 7).

At higher Rayleigh numbers there is evidence for transition to the theoretical upper bound of $1/3$ for the Nusselt number scaling exponent (see figure 4). This increase in the exponent for Nusselt number scaling with Rayleigh number from 0.2 towards $1/3$ occurs with the development of unsteady flow in the enclosure. Unsteady flow develops above a critical Rayleigh number in the range $3.5 \times 10^8 < Ra < 8.5 \times 10^8$, which is independent of aspect ratio (see figure 9).

In enclosures with large aspect ratios $D/L > 1$ (i.e. tall, slender enclosures), the critical Rayleigh number for transition from diffusion dominated to convection dominated flow is independent of aspect ratio. This likely occurs as a result of the top boundary being sufficiently far from the bottom boundary to wield no influence on the horizontal convection quantities monitored in this study.

REFERENCES

- CHIU-WEBSTER, S., HINCH, E.J. and LISTER, J.R., (2008), "Very viscous horizontal convection", *J. Fluid Mech.*, **611**, 395-426.
- HUGHES, G.O. and GRIFFITHS, R.W., (2008), "Horizontal convection", *Annu. Rev. Fluid Mech.*, **40**, 185-208.
- MULLARNEY, J.C., GRIFFITHS, R.W. and HUGHES, G.O., (2004), "Convection driven by differential heating at a horizontal boundary", *J. Fluid Mech.*, **516**, 181-209.
- NIEMELA, J.J. and SREENIVASAN, K.R., (2003), "Confined turbulent convection", *J. Fluid Mech.*, **481**, 355-384.
- PAPARELLA, F. and YOUNG, W.R., (2002), "Horizontal convection is non-turbulent", *J. Fluid Mech.*, **466**, 205-214.
- SHEARD, G.J., FITZGERALD, M.J. and RYAN, K., (2009), "Cylinders with square cross section: wake instabilities with incidence angle variation", *J. Fluid Mech.*, **630**, 43-69.
- SHEARD, G.J., LEWEKE, T., THOMPSON, M.C. and HOURIGAN, K., (2007), "Flow around an impulsively arrested circular cylinder", *Phys. Fluids*, **19**(8), 083601.
- SIGGERS, J.H., KERSWELL, R.R. and BALMFORTH, N.J., (2004), "Bounds on horizontal convection", *J. Fluid Mech.*, **517**, 55-70.
- WUNSCH, C. and FERRARI, R., (2004), "Vertical mixing, energy, and the general circulation of the oceans", *Annu. Rev. Fluid Mech.*, **36**, 281-314.